

## Magnetic-field-induced localization in degenerately doped *n*-type Ge

P. F. Hopkins, M. J. Burns,\* A. J. Rimberg, and R. M. Westervelt

*Division of Applied Sciences and Department of Physics, Harvard University, Cambridge, Massachusetts 02138*

(Received 21 November 1988; revised manuscript received 9 March 1989)

An experimental study is presented of the metal-to-insulator transition induced by moderate magnetic fields (to 7 T) and low temperatures (to  $\sim 100$  mK) in uncompensated, degenerately doped *n*-type Ge with Sb donors. The low-temperature ( $T < 1$  K) transverse and longitudinal magnetoresistance both increase strongly by as much as a factor of  $\sim 1000$  above a characteristic field  $H_c$ , with the temperature and field dependence  $\rho \propto \exp(bH^2/T^{1/4})$ . The measured Hall coefficient changes by less than a factor of  $\sim 4$  over the same range of magnetic field. Thus the apparent mobility decreases strongly above the metal-insulator transition, while the apparent carrier concentration changes relatively little, in contrast to magnetic freeze-out, in which the carrier concentration decreases. Careful checks of sample homogeneity argue against the possible influences of nonuniform dopant concentration.

### I. INTRODUCTION

Magnetic fields can produce interesting electronic phenomena in doped semiconductors.<sup>1-4</sup> The competition between the electron-donor-ion (*e-d*) interactions and electron-electron (*e-e*) interactions can result in a range of different phenomena depending on the relative strength of these terms. When the electron-ionized-donor interaction dominates, as for nondegenerately doped semiconductors, compression of the electronic wave functions onto isolated impurity ions by strong magnetic fields increases the donor binding energy. Consequently, the thermally excited carrier concentration is reduced in strong magnetic fields as the electrons become more strongly bound onto single donor impurity ions; we refer to this case as simple magnetic freeze-out.<sup>5</sup> The effects of magnetic freeze-out on electronic transport are a large increase in both the magnetoresistance and the Hall coefficient  $R_H$ , corresponding to a large reduction in carrier concentration. In degenerately doped semiconductors, the impurity wave functions overlap and *e-e* interactions become important. For this case it is not clear at the outset whether *e-d* or *e-e* interactions dominate. For sufficiently strong fields one does expect a type of magnetic freeze-out in degenerately doped semiconductors, driven by the compression of impurity wave functions, but the physical situation for this case is more complex than for simple freeze-out.<sup>1,2</sup>

For doped semiconductors in magnetic fields weaker than those required for magnetic freeze-out, other disorder-induced phenomena are possible. A possible transition in degenerately doped semiconductors is localization, where the apparent carrier concentration, measured by the Hall effect, stays relatively constant, but the conductivity decreases strongly due to a decreasing mobility. Throughout this paper we use the term localization in the experimental sense to refer to this type of metal-insulator transition. Localization is also sometimes used in the theoretical sense to refer to noninteracting

electronic theory which predicts this type of transition.<sup>6</sup> Note, however, that it is possible that a localization transition (in the experimental sense) may occur in theoretical cases where electron-electron interactions are important.<sup>7-9</sup>

Recent scaling theories,<sup>7-9</sup> including both disordered Coulomb interactions and single-particle "localization" terms, address the behavior of the conductivity near the metal-insulator transition in strong magnetic fields. However, no corresponding theory for the Hall effect has been presented to our knowledge. It is important to note that the mathematical form of some Coulomb interaction terms in these theoretical approaches is similar to single-particle localization terms.

Finally, in the limit of no disorder, where the positive charge is assumed to be uniformly spread out in space and the *e-e* interaction dominates, collective phenomena such as spin-density waves, charge-density waves, and Wigner crystallization have been predicted to occur.<sup>3,4,10,11</sup> Novel transport phenomena<sup>3,4</sup> can be associated with these different electronic states. In degenerately doped semiconductors, with a strong impurity potential, collective electronic phenomena may also occur but any collective state present must be heavily disordered, and the theory for this case is difficult.<sup>3,4</sup> Experimentally, any heavily disordered collective state would be difficult to distinguish from single-particle behavior.

In recent years, experiments have been performed to study electronic phenomena induced by magnetic fields in doped semiconductors. Two useful parameters which characterize these transitions are  $\gamma = h\omega_c/4\pi E_D$ , the ratio of the magnetic zero-point energy of a free electron  $h\omega_c/4\pi$  to the donor binding energy  $E_D$ , and  $\xi = h\omega_c/2\pi E_F$ , the ratio of the cyclotron energy  $h\omega_c/2\pi$  to the Fermi energy in zero field. Values of  $\gamma > 1$ , the "strong" field regime, correspond to strong compression of the donor wave functions, and favor magnetic freeze-out.<sup>5</sup> The condition  $\xi > 1$  corresponds to the quantum limit where all electrons are in the lowest Landau level at

$T=0$  and marks the point at which the Fermi energy starts to decrease with increasing field strength. For no disorder, collective phenomena are predicted to occur in the quantum limit. However, the reduction of the Fermi energy by the magnetic field increases the influence of disorder, favoring magnetic-field-induced localization.

Narrow-gap semiconductors are natural candidates for such experiments, because large ratios  $\gamma$  and  $\xi$  can be obtained in relatively modest fields. Magnetoresistance and Hall data have been reported for InSb,<sup>12,13</sup>  $\text{Hg}_{1-x}\text{Cd}_x\text{Te}$ ,<sup>13-18</sup> and InAs,<sup>19</sup> all in the strong-field regime. Experiments on InSb are generally considered to be examples of magnetic freeze-out. The interpretation of data for  $\text{Hg}_{1-x}\text{Cd}_x\text{Te}$ , however, is controversial and has been used as evidence for both magnetic freeze-out<sup>13</sup> and Wigner crystallization<sup>14,15</sup> as well as a correlated "viscous liquid."<sup>16</sup> Recent experiments on InAs have been used as evidence for a proposed "Hall-insulator" state,<sup>19</sup> for which the Hall effect remains metallic for fields above the metal-insulator transition, while the magnetoresistance increases strongly. Interpretations of some of these data, however, are complicated by controversy over material characteristics of the samples.<sup>20</sup> Magnetoresistance and Hall-effect measurements in the weak-field regime on Si:As (Ref. 21) have been made approaching, but not observing, the transition from both the insulating and the metallic side and have been discussed in terms of variable-range hopping and magnetic tuning of the localization exponent.

In this paper we present an experimental study of low-temperature electronic transport in uncompensated, degenerately doped  $n$ -type Ge:Sb in modest magnetic fields. We find a magnetic-field-induced metal-insulator transition for  $\gamma < 1$  in which the transverse and longitudinal magnetoresistance both increase by as much as 3 orders of magnitude and exhibit variable-range hopping behavior  $\rho \propto \exp(bH^2/T^{1/4})$ . However, the apparent carrier concentration from the Hall-effect measurements changes relatively little over the same range of field, by a factor less than  $\sim 4$ . Thus simple magnetic freeze-out does not occur. This lack of change in the carrier concentration, together with the relatively small magnetic fields needed to induce the metal-insulator transition, are evidence for field-induced localization, as discussed below. Preliminary accounts of this work have appeared elsewhere.<sup>22,23</sup>

## II. EXPERIMENTAL DETAILS

The material used for this study was uncompensated Czochralski-grown Ge degenerately doped with Sb donors, obtained from Eagle-Picher. The three samples discussed in this paper, 1-3, were cut from two different Ge crystals; their measured characteristics are summarized in Table I. The donor concentration  $N_D$  indicated was determined by room-temperature resistivity measurements<sup>24</sup> and checked by room-temperature Hall measurements. For samples 1 and 3,  $N_D$  is near the critical concentration  $n_c \sim 1.5 \times 10^{17} \text{ cm}^{-3}$  for the metal-insulator transition in zero field, while for sample 2 the donor concentration is a factor  $\sim 1.7$  above  $n_c$ . The samples were cut with a diamond saw with all faces perpendicular to  $\langle 100 \rangle$  crystal axes, lapped, and etched in 3:1 (by volume) concentrated  $\text{HNO}_3$  to HF. Electrical contacts were made using Sn solder, either nominally pure or doped with Sb; typical measured contact resistances were 2-4  $\Omega$  at low temperatures. Samples 1 and 2 were prepared in a virtual-contact Hall bar geometry<sup>25,26</sup> with dimensions  $10 \times 1.7 \times 0.56$  and  $6.4 \times 1.1 \times 0.22 \text{ mm}^3$ , respectively, and sample 3 was prepared in a special eight-contact van der Pauw geometry<sup>27</sup> as discussed below. For samples 1 and 2 current contacts were attached along opposite 1.7- and 1.1-mm ends, and three voltage contacts were arranged along opposite sides to permit virtual-contact Hall measurements, as well as four-terminal resistance measurements. Care was exercised to mount the samples stress free.

Low-temperature electrical measurements were made in a Oxford Instruments Model 200 dilution refrigerator to temperatures  $T \sim 100 \text{ mK}$  and magnetic fields  $H = 7 \text{ T}$  using conventional low-noise ac ( $\sim 25 \text{ Hz}$ ) lock-in-amplifier techniques. The data were taken by controlling the temperature and ramping the field  $H$ . To avoid eddy-current heating of the sample, the ramping rates were typically limited to  $dB/dt < 0.07 \text{ T/min}$ . Care was taken to limit power dissipation in the samples to  $\sim 10^{-12} \text{ W}$  to avoid heating and to remain in the linear portion of the current-voltage characteristics. Longitudinal (current parallel to  $\mathbf{H}$ ), and transverse magnetoresistance measurements were made on each sample with the field  $\mathbf{H}$  oriented along a  $\langle 100 \rangle$  axis by rotating the sample through  $90^\circ$ . Because the magnetoresistance signal was

TABLE I. Parameter chart for the three Ge:Sb samples whose data appear in this paper. The dopant concentration  $N_D$  was obtained from  $T = 300 \text{ K}$  measurements to  $\pm 10\%$ . The low-temperature carrier concentration  $n$  and Hall mobility  $\mu_H$  were found from resistance and low-field Hall measurements at temperatures  $T = 400 \text{ mK}$  for samples 1 and 2 and  $T = 225 \text{ mK}$  for sample 3 using a Hall factor of 1. The zero-temperature critical field was calculated as discussed in the text.

Sample	Dimensions (mm <sup>3</sup> )	$N_D$ ( $10^{17} \text{ cm}^{-3}$ )	$n$ ( $10^{17} \text{ cm}^{-3}$ )	$\mu_H$ (cm <sup>2</sup> /V s)	$H_c$ (T)
1	$10 \times 1.7 \times 0.56$	1.6	1.3	440	3.8
2	$6.4 \times 1.1 \times 0.22$	2.6	2.2	620	5.2
3	(see Fig. 1)	1.6	1.1	420	

as much as a factor  $\sim 10^4$  larger than the Hall signal, low-noise Hall measurements posed special difficulties. These were minimized both by using a five-contact Hall bar geometry with a virtual Hall contact to null-out unwanted magnetoresistance pickup, and by subtracting two data sets with the magnetic field reversed to remove any residual magnetoresistance signal not canceled by the virtual-contact technique.

Inhomogeneity of the impurity concentration can be a serious problem in heavily doped Czochralski crystals, both as slow variations in donor concentration  $N_D$  across the crystal, and as narrow, planar impurity striations which form perpendicular to the growth direction,  $\langle 100 \rangle$  for our crystals. Impurity striations can be difficult to detect by conventional methods such as spreading resistance measurements, because the length scales can be as small as  $1\text{--}10\ \mu\text{m}$ . We took two precautions to guard against inhomogeneity in our samples, described below.

First, we screened crystals for striations and large-scale inhomogeneities by cutting a thin, square sample with all faces perpendicular to  $\langle 100 \rangle$  axes, and with the known growth direction along one side of the square. Contacts were attached to the four corners, and the sample was driven through the metal-insulator transition at low temperatures ( $T < 0.5\ \text{K}$ ) by a magnetic field  $\mathbf{H}$  oriented perpendicular to the square face. The isotropy of the dopant

concentration was tested by comparing two sets of four-terminal magnetoresistance measurements with the leads rotated by  $90^\circ$ , which should be identical by crystal symmetry. As seen below, the resistance of the sample increases strongly above the density-dependent transition field  $H_c$ . Hence, for fields above  $H_c$  for less dense parts of the striations, but not yet above  $H_c$  for more dense parts, the resistance perpendicular to the striations is much larger than the parallel resistance. This method is extremely sensitive to striations and detected those not found with spreading resistance measurements. For the samples discussed below, the measured anisotropy in the transition field,  $\Delta H_c$ , was less than 3.5%, implying a comparable limit on variation in the dopant concentration.

Highly conducting paths due to nonuniform dopant concentration can also lead to incorrect Hall measurements by effectively shorting the Hall contacts. The second precaution we took against such preferred current paths,<sup>28</sup> was to make a special eight-contact sample (3) in the van der Pauw geometry<sup>27</sup> illustrated in Fig. 1. This sample consists of two sets of four van der Pauw contacts, labeled 1 and 2 in Fig. 1, one set aligned with the crystal growth direction and the other rotated by  $45^\circ$ . Notches were cut as indicated to relieve possible contact-related effects such as stress and current path inhomogeneities near the contacts. The isotropy checks described above, and van der Pauw measurements of the transverse magnetoresistance and the Hall coefficient were all repeated twice for this sample, using both sets of contacts. Data from this special sample confirm those in the Hall bar samples as discussed below in Sec. III.

### III. EXPERIMENTAL RESULTS

Logarithmic plots of the measured transverse and longitudinal magnetoresistance  $\rho_{xx}$  and  $\rho_{zz}$  versus magnetic field  $\mathbf{H}$  are shown in Figs. 2(a) and 2(b) for sample 1, and in Figs. 3(a) and 3(b) for sample 2, at various temperatures between  $T = 80$  and  $T = 450\ \text{mK}$ . The data in Fig. 2 show clear evidence of a metal-insulator transition in which both  $\rho_{xx}$  and  $\rho_{zz}$  increase above a characteristic field  $H_c$  by as much as a factor of  $\sim 2000$ . The magnetoresistance changes from a weakly field- and temperature-dependent metallic regime below  $H_c$  to an activated hopping conduction regime above  $H_c$ . The data shown in Figs. 3(a) and 3(b) for the more heavily doped sample 2 are in qualitative agreement with Figs. 2(a) and 2(b); however, the characteristic field  $H_c$  is increased and the size of the resistance rise is decreased, as expected for higher donor concentration. By extrapolating the temperature-dependent conductivity in the metallic regime to  $T = 0$ , we find<sup>23</sup> a metal-insulator transition of the form  $\sigma(H, T = 0) \propto (H_c - H)^\xi$  with  $\xi \approx 1$ . The characteristic transition fields obtained<sup>23</sup> by linearly extrapolating  $\sigma(H, T = 0)$  to zero are  $H_c \approx 3.8\ \text{T}$  for sample 1 and  $H_c \approx 5.2\ \text{T}$  for sample 2, so that  $H_c$  increases roughly linearly with dopant density.

The low-field ( $H < 2\ \text{T}$ ) magnetoresistance shows many characteristics previously observed in either Ge:Sb (Refs. 29–31) or in Si:P.<sup>32,33</sup> Because an analysis of our data in

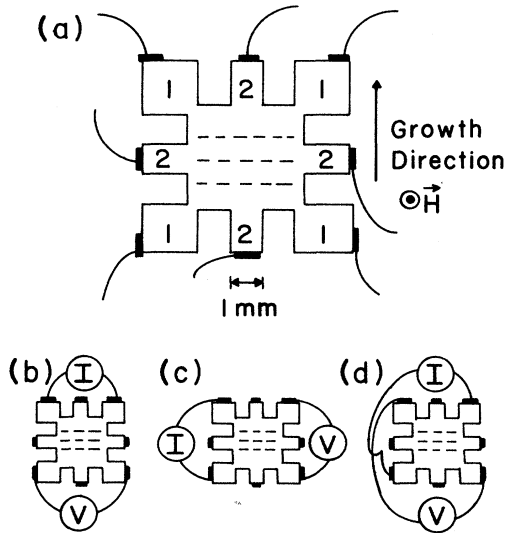


FIG. 1. (a) Eight-contact van der Pauw sample 3 (outer dimensions  $6.35 \times 6.35 \times 0.32\ \text{mm}^3$  and all faces  $\{100\}$ ) with two sets of four contacts, rotated  $45^\circ$  with respect to each other and labeled 1 and 2, which was used for homogeneity checks. Macroscopic and microscopic inhomogeneities, including impurity striations which are indicated by dashed lines, were screened by looking for anisotropies in the magnetoresistance measurements with lead configurations (b) and (c). Two independent sets of magnetoresistance and Hall measurements on contact sets 1 and 2 were used as a further homogeneity check and to test for possible current paths between Hall contacts; the Hall lead configuration for contact set 1 is shown in (d).

the low-field regime has been published,<sup>23</sup> and is the subject of another paper,<sup>34</sup> we only summarize the results here. At higher temperatures and low fields the magnetoresistance is negative, which is characteristic of weak localization.<sup>35</sup> As the temperature is reduced, and at higher fields in the metallic regime, a positive magnetoresistance with the temperature dependence  $\Delta\rho/\rho \propto T^{1/2}$  due to disordered Coulomb interactions dominates weak localization effects. At the lowest temperatures, where localization effects are relatively small, the magnetoresistance crosses over from a  $\Delta\rho/\rho \propto H^2$  to a  $\Delta\rho/\rho \propto H^{1/2}$  dependence at a characteristic field close to

that calculated for disordered Coulomb interactions.<sup>36</sup>

The high-field ( $H > H_c$ ) magnetoresistance is characterized by a strong increase in both  $\rho_{xx}$  and  $\rho_{zz}$  at low temperatures by as much as a factor of  $\sim 2000$  for sample 1 at  $T = 80$  mK and  $H = 7$  T. Comparisons of transverse and longitudinal magnetoresistance  $\rho_{xx}$  and  $\rho_{zz}$  in Figs. 1 and 2 show that this increase is nearly isotropic as expected for hopping conduction.

The temperature dependence of the resistivity of sample 1 over the range 80 mK–4.0 K is shown in Fig. 4; the data points were obtained from Fig. 2(a) and from additional higher-temperature measurements. In Fig. 4

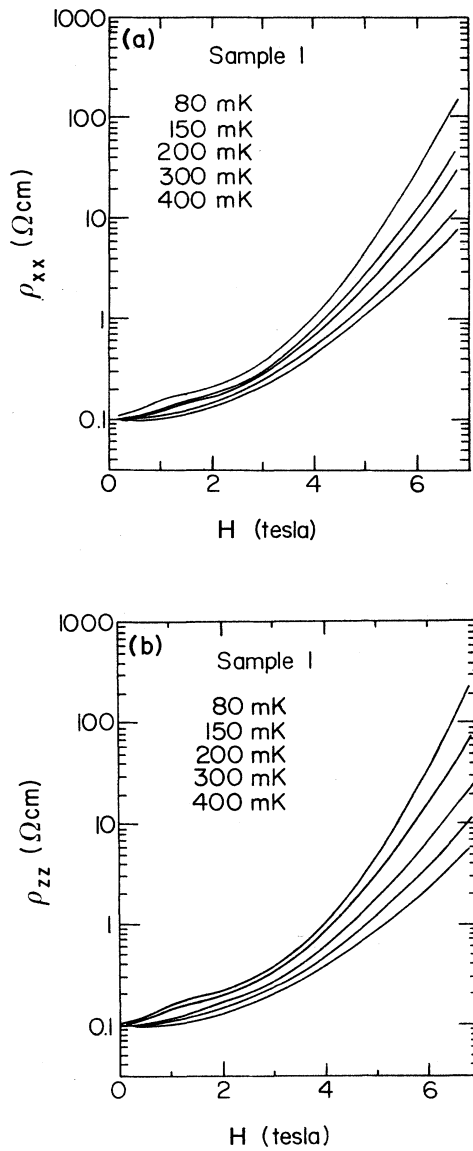


FIG. 2. (a) Logarithm of the transverse resistivity  $\rho_{xx}$  vs magnetic field  $H$  for sample 1 at the temperatures indicated; (b) logarithm of the longitudinal resistivity  $\rho_{zz}$  vs  $H$  for the same sample at the same temperatures.

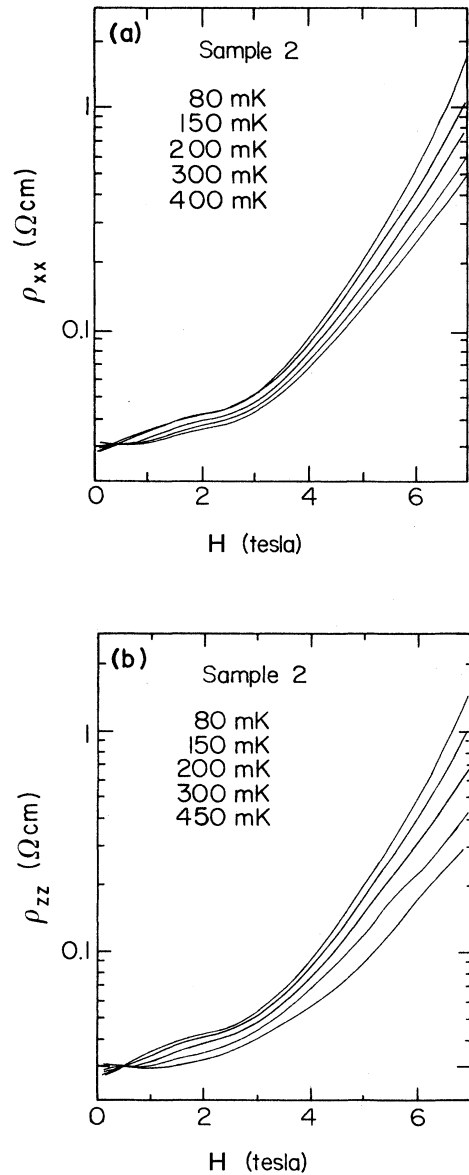


FIG. 3. (a) Logarithm of  $\rho_{xx}$  vs  $H$  for sample 2 at the temperatures indicated; (b) logarithm of  $\rho_{zz}$  vs  $H$  for the same sample at the same temperatures.

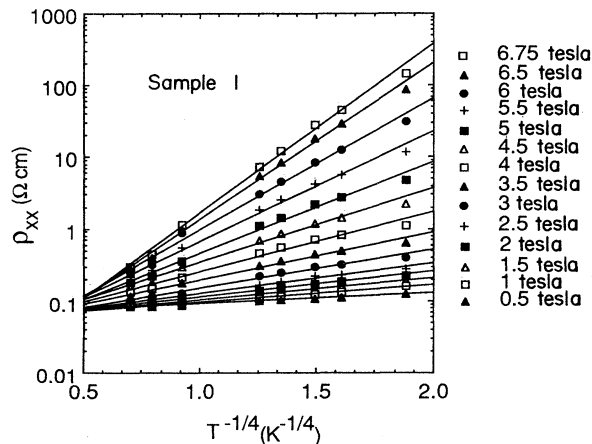


FIG. 4. Temperature dependence of transverse resistivity for the lower doped sample 1. Plotted is  $\log_{10}\rho_{xx}$  vs  $T^{-1/4}$  for various magnetic field values, demonstrating for magnetic fields  $H > H_c$  the form  $\rho \propto \exp(T_0/T)^{1/4}$ , characteristic of variable-range hopping. Least-squares fits to the data are shown.

$\log_{10}\rho_{xx}$  is plotted versus  $T^{-1/4}$  for various magnetic field strengths. The data for  $T=80$  mK lie below the fitted curves suggesting some sample heating. The low-field data for  $H < H_c$  correspond to the metallic side of the transition and fit  $\Delta\rho/\rho \propto T^{1/2}$  as discussed above. Above the critical field  $H_c \approx 3.8$  T, the data shows activated behavior  $\rho = \rho_0(H)\exp(T_0/T)^{1/4}$  characteristic of three-dimensional (3D) variable-range hopping conduction.<sup>2</sup> Theories of 3D variable-range hopping incorporating  $e-e$  Coulomb interactions predict<sup>1</sup> the dependence  $\rho \propto \exp(T_0/T)^{1/2}$  at sufficiently low temperatures. However, this temperature dependence does not fit our data as well as  $\rho \propto \exp(T_0/T)^{1/4}$  below  $T=1$  K as shown in Fig. 4. Least-squares fits to all the data, shown in Fig. 4, determine the magnetic field dependence of  $T_0(H)$ , which is plotted in Fig. 5. As shown,  $T_0(H)$  exhibits a sharp

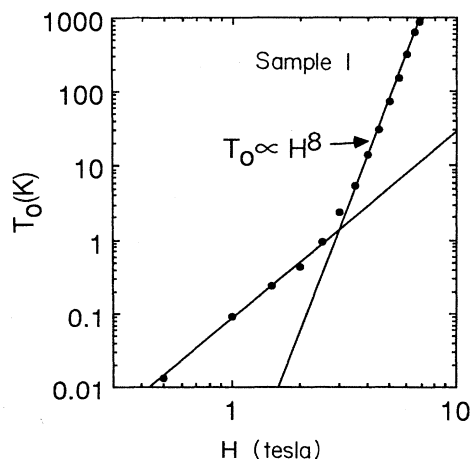


FIG. 5. Log-log plot of  $T_0(H)$  vs  $H$  data obtained from slopes of fitted curves in Fig. 4. Above the transition field  $H_c \sim 3.8$  T,  $T_0 \propto H^8$ , yielding the form  $\rho \propto \exp(bH^2/T^{1/4})$ .

break in slope near  $H_c$ . For fields above  $H_c$ , the field dependence of  $T_0$  is accurately  $T_0 \propto H^8$  as shown. Thus the temperature and magnetic field dependence of the resistivity in the hopping regime is of the form  $\rho \propto \exp(bH^2/T^{1/4})$  where  $b$  is a constant; this magnetic field dependence is characteristic of hopping models in the weak-field regime.<sup>1</sup>

The normalized Hall coefficients  $R_H = \rho_{xy}/H$  for samples 1 and 2, are shown in Figs. 6(a) and 6(b), respectively, measured over the given temperatures and the same range of fields as for Figs. 2 and 3. In these plots a constant apparent carrier density would correspond to a horizontal straight line. The striking feature of these data is the absence of the strong metal-insulator transition found in the magnetoresistance data, Figs. 2 and 3: the Hall coefficient for sample 1 at  $T=150$  mK increases only by a factor  $\sim 4$ , while  $\rho_{xx}$  increases by a factor  $\sim 500$  in Fig. 2(a). For sample 2 at 80 mK,  $R_H$  increases by a factor  $\sim 2.5$  while  $\rho_{xx}$  increases by a factor  $\sim 50$  in Fig. 3(a). Furthermore, the Hall coefficient shows little temperature dependence between  $T \sim 100$  and  $T \sim 400$  mK, both at low and high fields, as expected for the metallic regime. These data imply that the apparent carrier concentration changes relatively little across the metal-insulator

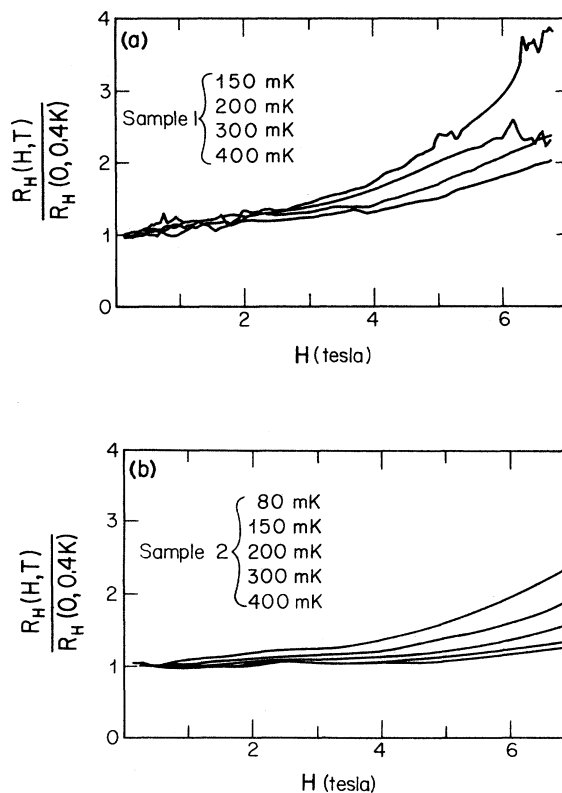


FIG. 6. Measured Hall coefficient  $R_H = \rho_{xy}/H$  at the temperatures indicated for (a) sample 1, and (b) sample 2. Here  $R_H$  is normalized to the value at zero field and  $T=400$  mK. Note the absence of signs of the metal-insulator transition present in the corresponding magnetoresistance data, Figs. 2 and 3.

transition. Using the virtual contact Hall bar geometry, the Hall voltage for sample 2 was at least ten times the residual magnetoresistance voltage, so the systematic error due to magnetoresistance signal is small. The systematic error for sample 1 was larger, comparable to the noise shown, due to the larger magnetoresistance pickup.

While the Hall bar geometry is very effective in reducing magnetoresistance pickup in the Hall signal, it is susceptible to the effects of dopant inhomogeneity. In particular, the data above could in principle be explained by a high-donor-concentration conducting path between the fixed Hall contacts, or between the current contacts. In order to test for dopant inhomogeneity, we repeated the transverse magnetoresistance and Hall measurements at  $T=225$  mK on a special sample (3) cut from the same crystal as 1, but in a van der Pauw geometry with two pairs of four contacts rotated by  $45^\circ$  as described in Sec. II and illustrated in Fig. 1. Four contacts at the corners of a square were used to test for effects of inhomogeneities such as impurity striations in the magnetoresistance, by rotating the current and voltage leads  $90^\circ$ . However, eight contacts are necessary to test for the effects of inhomogeneity in the Hall signal, because the Hall resistance measured with only four contacts is independent of the choice of leads for any impurity distribution by the reciprocity theorem.

The results of an isotropy check of the transverse magnetoresistance  $\rho_{xx}$  are shown in Figs. 7(a) and 7(b): for Fig. 7(a) the four contacts were chosen symmetrically  $45^\circ$  from the plane along which impurity striations form, as indicated in the inset, while in Fig. 7(b), the contacts were in the plane of striations. Two curves are shown for each figure, which correspond to rotating the current and voltage leads  $90^\circ$ . Both Figs. 7(a) and 7(b) show a metal-insulator transition in agreement with the Hall bar data, shown in Fig. 2. For the symmetric choice of contacts in Fig. 7(a), both curves practically coincide, evidence for the absence of large-scale inhomogeneities in this sample. For the choice of contacts in Fig. 7(b), the magnetoresistance curve with voltage contacts in the plane of the striations yields a slightly lower resistance at high fields. This anisotropy was used to estimate the magnitude of the variation of donor concentration between striations as described in Sec. II. By extrapolating the conductivity to zero temperature in the metallic regime, we estimate an anisotropy of  $\sim 3.5\%$  in  $H_c$  for this sample, from which we infer a comparable variation in impurity concentration within striations.

Hall data taken for the special van der Pauw sample 3 with both contact orientations are shown in Figs. 8(a) and 8(b). As shown, the normalized Hall coefficient measured for both sets of contacts agree accurately with each other, and with the data from the Hall bar sample 1 shown in Fig. 6(a): all show little evidence of the metal-insulator transition in the magnetoresistance. The agreement of the Hall data for both orientations Figs. 8(a) and 8(b), and for the Hall bar sample, Fig. 6(a), provides strong evidence against the possible influence of dopant inhomogeneities on the data. The disadvantage of the van der Pauw geometry is the large magnetoresistance pickup at high fields where the magnetoresistance  $R_{xx}$  is larger

than the Hall resistance  $R_{xy}$  by a factor as large as  $\sim 250$ ; this pickup was reduced by subtracting Hall data taken with reversed field  $H$ . The large temperature dependence of  $\rho_{xx}$  above the transition demanded careful temperature control during the time required to reverse the magnetic

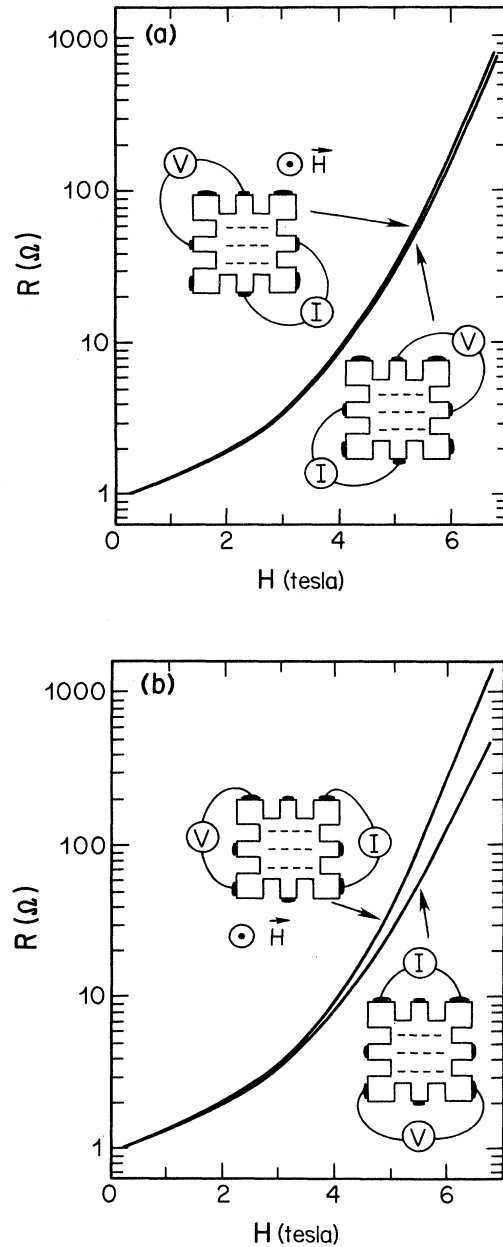


FIG. 7. van der Pauw transverse magnetoresistance measurements for sample 3 (see Fig. 1) at  $T=225$  mK for (a) contact set 2 symmetric with respect to possible impurity striations indicated as the dashed lines, and (b) contact set 1 aligned with the striations. The current and voltage connections for each measurement are indicated in the insets. In each figure, the two magnetoresistance curves were normalized to each other at zero field to more clearly show their anisotropy.

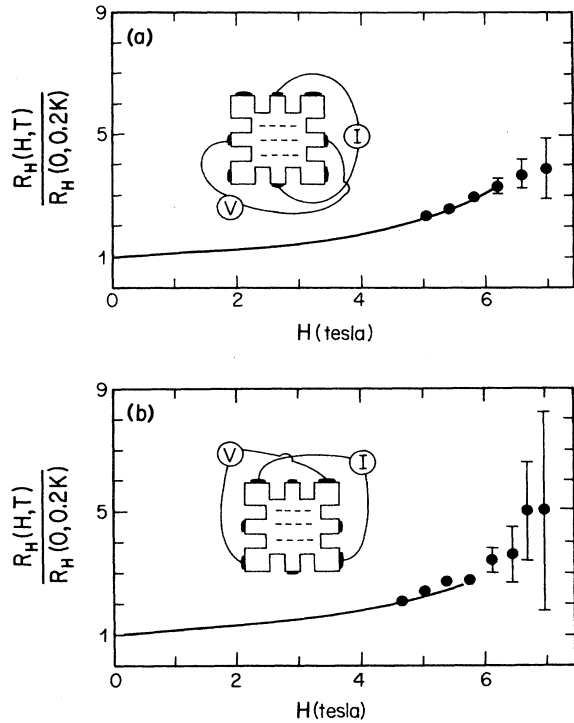


FIG. 8. van der Pauw measurements of the normalized Hall coefficient  $R_H$  for sample 3 (see Fig. 1) at  $T=225$  mK for (a) contact set 1, and (b) contact set 2. The current and voltage connections are indicated in the insets. The smooth curves were obtained by subtracting reversed magnetic field sweeps using conventional temperature control, whereas the data points with error bars were measured using the magnetoresistance to control the sample temperature with greater accuracy between field reversals.

field to allow accurate cancellation of magnetoresistance pickup in the Hall signal. To accomplish this, the measured magnetoresistance was used as a thermometer to control the temperature to within an error  $\Delta T < 0.1$  mK. Estimates of the error associated with this procedure are shown as the error bars in the Hall coefficient  $R_H$  at high fields in Figs. 8(a) and 8(b). At lower fields where the magnetoresistance is smaller, Hall data were recorded without special temperature control, and are shown as the continuous curve.

#### IV. DISCUSSION

In summary, we find a magnetic-field-induced metal-insulator transition above which the magnetoresistance increases strongly, with the form  $\rho \propto \exp(bH^2/T^{1/4})$ , while the Hall coefficient changes relatively little. The simple interpretation of this data for a uniform conductor would be that the mobility decreases strongly while the carrier concentration remains essentially constant. These characteristics are evidence for field-induced localization and are in contradiction to simple magnetic freeze-out, for which the carrier concentration decreases abruptly at the transition. Careful homogeneity checks confirm these results and argue against the possible influence of impuri-

ty striations or other dopant inhomogeneities.

Magnetic-field-induced metal-insulator transitions have been previously observed in degenerately doped semiconductors other than Ge. As noted above, these metal-insulator transitions can be characterized by two parameters:  $\gamma = \hbar\omega_c/4\pi E_D$  and  $\xi = \hbar\omega_c/2\pi E_F$ . Large values of the first parameter  $\gamma$  favor magnetic freeze-out while large values of the second parameter  $\xi$  favor field-induced localization or collective phenomena depending on the amount of disorder. For the cited experimental work in narrow gap semiconductors,<sup>12-19</sup> the magnetic-field-induced metal-insulator transitions occur at magnetic fields where both ratios are large:  $\gamma > 1$  and  $\xi > 1$ . The interpretation of these data can be difficult, because field-induced localization, collective phenomena, and magnetic freeze-out are all possible. For example, metal-insulator transitions were reported<sup>13-18</sup> in  $\text{Hg}_{1-x}\text{Cd}_x\text{Te}$  at magnetic fields corresponding to  $\gamma \sim 7-150$ , with  $\xi \sim 6-10$ , and interpreted alternately as evidence for collective electron motion, Wigner crystallization, and magnetic freeze-out. In InAs a transition was observed<sup>19</sup> for  $\gamma \sim 3$ , with  $\xi \sim 1$ , and interpreted as evidence for a "Hall insulator." Data for InSb (Refs. 12 and 13) with  $\gamma \sim 1-30$ , and  $\xi \sim 1-5$  have a consistent interpretation as magnetic freeze-out.

In contrast to this previous work, the magnetic-field-induced metal-insulator transition reported here for degenerately doped Ge occurs at relatively weak fields ( $\gamma \sim 0.2$ ) which are nevertheless in the quantum limit ( $\xi \sim 2$ ). Thus simple magnetic freeze-out is not expected, but field-induced localization and collective phenomena are possible. The carrier concentration in  $n$ -type Ge is expected to freeze out in sufficiently strong magnetic fields; the condition  $\gamma=1$  for shallow donors in Ge requires  $H \sim 25$  T. Similar ( $\gamma \sim 0.5$  and  $\xi \sim 1$ ) values for these parameters were found at the metal-insulator transition for compensated GaAs,<sup>37</sup> but the Hall effect was not measured.

Several authors have studied a different problem: the dependence of the Hall effect as the donor concentration is varied about the metal-insulator transition in essentially zero magnetic field. For compensated Ge:Sb in small magnetic fields ( $H \sim 0.3$  T) and at low temperatures ( $T \sim 8$  mK) Field *et al.*<sup>31</sup> find that the conductivity and the apparent carrier concentration decrease by comparable factors  $\sim 3$  below the normal metallic value near the critical donor concentration  $n_c$  in zero magnetic field, hence the mobility changes relatively little. Similar behavior has also been reported<sup>38</sup> for the metal-insulator transition in  $\text{Bi}_x\text{Kr}_{1-x}$ . These data have been used as evidence against localization for the metal-insulator transition with donor concentration in zero magnetic fields. However, recent experiments in Si:As (Ref. 21) in the low magnetic field limit do not find a divergence in the Hall coefficient, and are in agreement with localization theory predictions.

Both single-particle localization terms and electron-electron interactions can be important at the metal-insulator transition. Finkelstein<sup>7</sup> and Castellani *et al.*<sup>8,9</sup> have developed scaling theories for the conductivity near the transition which include both disordered Coulomb in-

teraction and single-particle localization terms. However, these models do not address the behavior of the Hall conductivity, and do not include the magnetic field from the outset. Coulomb interaction theory<sup>39</sup> in the limit of zero magnetic field predicts that the Hall coefficient diverges at the metal-insulator transition, whereas the scaling theory of localization,<sup>6</sup> neglecting Coulomb interactions and magnetic field effects, predicts that the Hall coefficient approaches the metal-insulator transition from the metallic side with little change. The absence of a divergence in the Hall coefficient, evidence for experimental localization, is seen in our data above for the magnetic-field-induced metal-insulator transition in Ge:Sb. However, it is difficult to justify the neglect of Coulomb interactions for our case, and a theory of the Hall effect including both disordered Coulomb interactions and single-particle localization terms is needed.

A fundamental characteristic of metal-insulator transitions in disordered materials is spatial breakup of the current path near the transition; on the insulating side of this transition, hopping conduction is expected at finite temperatures. For a model in which the magnetic field converts electronic states at the Fermi level from extended to localized states, the expected behavior is variable-range hopping.<sup>3</sup> In the weak magnetic field regime, the predicted magnetoresistance for this case is approximately isotropic and varies with temperature as  $\rho_{xx} \propto \exp[(T_0(H)/T)^{1/4}]$ .<sup>2</sup> Many variable-range hopping models<sup>1</sup> predict  $T_0 \propto H^8$  in the weak magnetic field regime. The lack of anisotropy, the temperature dependence, and the magnetic field dependence for variable-range hopping are all consistent with the data shown in Figs. 4 and 5.

The Hall resistance for variable-range hopping is difficult to calculate, and there does not appear to be a consensus on the result for the rapid hopping limit appropriate to our experiments.<sup>40-42</sup> However, the Hall resistivity  $\rho_{xy}$  in these models is much smaller than  $\rho_{xx}$ , typically<sup>3</sup> increasing with  $\rho_{xx}$  as  $\rho_{xy} \propto \rho_{xx}^b$  with  $b \cong \frac{1}{2}$  in the low magnetic field limit. This dependence suggests the form  $\rho_{xy} \propto \exp\{b(H)[T_0(H)/T]^{1/4}\}$ . This temperature dependence is consistent with our Hall data reported

above; our experimental value of  $b(H)$  for  $H = 6$  T is  $b(H) \cong 0.32$  and decreases with  $H$ . For Si:As in relatively weak fields,  $\gamma < 0.1$ , Koon *et al.*<sup>21</sup> found that  $b(H)$  decreased with magnetic field from the value  $b = 0.63$  obtained in the limit  $H \rightarrow 0$  and  $N_D \rightarrow n_c$ . This limit agrees with the theoretical value  $b = \frac{5}{8}$  of Gruenewald *et al.*<sup>40</sup>

Both the value and field dependence of  $b(H)$  from our data for Ge are consistent with extrapolated results for Si (Ref. 21) when plotted versus the normalized magnetic field  $\gamma$ , as defined above.

The anomalous behavior of the Hall coefficient reported here could also be interpreted as evidence for collective phenomena. An interesting possibility is that electron-electron interactions act to produce strongly correlated hopping. In this picture, the interactions impede localization of single electrons onto impurity sites so that the Hall coefficient remains metallic. This is a qualitative feature of some phenomenological models<sup>16,17,43</sup> of collective transport. However, although collective phenomena are possible in principle, they are not required to explain our experimental data.

In summary, our data for the field-induced metal-insulator transition in *n*-type Ge are evidence for magnetic-field-induced localization in which the Hall coefficient changes relatively little, while the magnetoresistance increases sharply. Above the transition field, both the magnetoresistance and Hall resistance are in agreement with the predictions of variable-range hopping theory.

#### ACKNOWLEDGMENTS

We thank B. I. Halperin, G. A. Thomas, P. A. Lee, A. B. Fowler, and P. Stiles for helpful comments. Preliminary work was performed with technical assistance from Bruce Brandt at the Francis Bitter National Magnet Laboratory, supported at MIT by the National Science Foundation. One of us (P.F.H.) acknowledges support by IBM. This work was supported by the National Science Foundation under Grants No. DMR-85-08733 and No. DMR-86-14003.

\*Present address: Department of Physics, University of Florida, Gainesville, FL 32611.

<sup>1</sup>B. I. Shklovskii and A. L. Efros, *Electronic Properties of Doped Semiconductors* (Springer-Verlag, Berlin, 1984).

<sup>2</sup>N. F. Mott and E. A. Davis, *Electronic Properties in Non-Crystalline Materials*, 2nd ed. (Oxford University Press, Oxford, 1979).

<sup>3</sup>B. I. Halperin, in *Proceedings of the 18th International Conference on Low Temperature Physics, Kyoto, 1987* [Jpn. J. Appl. Phys. **26**, Suppl. 26-3, Pt. 3 (1987)].

<sup>4</sup>B. I. Halperin, in *Condensed Matter Theories*, edited by P. Vashista *et al.* (Plenum, New York, 1987), Vol. 2.

<sup>5</sup>Y. Yafet, R. W. Keyes, and E. N. Adams, J. Phys. Chem. Solids **1**, 137 (1956); R. W. Keyes and R. J. Sladek, *ibid.* **1**, 143 (1956).

<sup>6</sup>B. Shapiro and E. Abrahams, Phys. Rev. B **24**, 4025 (1981).

<sup>7</sup>A. M. Finkelstein, Zh. Eksp. Teor. Fiz. **84**, 168 (1983) [Sov.

Phys.—JETP **57**, 97 (1983)]; **86**, 367 (1984) [**59**, 212 (1984)].

<sup>8</sup>C. Castellani, C. DiCastro, P. A. Lee, and M. Ma, Phys. Rev. B **30**, 527 (1984).

<sup>9</sup>C. Castellani, G. Kotliar, and P. A. Lee, Phys. Rev. Lett. **59**, 323 (1987).

<sup>10</sup>V. Celli and N. D. Mermin, Phys. Rev. **140**, A839 (1965).

<sup>11</sup>W. G. Kleppman and R. J. Elliott, J. Phys. C **8**, 2729 (1975); H. Fukuyama, Solid State Commun. **26**, 783 (1978).

<sup>12</sup>S. Ishida and E. Otsuka, J. Phys. Soc. Jpn. **43**, 124 (1977); **46**, 1207 (1979).

<sup>13</sup>M. Shayegan, V. J. Goldman, H. D. Drew, N. A. Fortune, and J. S. Brooks, Solid State Commun. **60**, 817 (1986); M. Shayegan, V. J. Goldman, H. D. Drew, D. A. Nelson, and P. M. Tedrow, Phys. Rev. B **32**, 6952 (1985).

<sup>14</sup>G. Nimtz, B. Schlicht, E. Tyssen, R. Dornhaus, and L. D. Haas, Solid State Commun. **32**, 669 (1979).

<sup>15</sup>T. F. Rosenbaum, S. B. Field, D. A. Nelson, and P. B. Little-



- wood, Phys. Rev. Lett. **54**, 241 (1985).
- <sup>16</sup>J. P. Stadler, G. Nimtz, B. Schlicht, and G. Remenyi, Solid State Commun. **52**, 67 (1984).
- <sup>17</sup>M. Shayegan, H. D. Drew, D. A. Nelson, and P. M. Tedrow, Phys. Rev. B **31**, 6123 (1985).
- <sup>18</sup>V. J. Goldman, M. Shayegan, and H. D. Drew, Phys. Rev. Lett. **57**, 1056 (1986).
- <sup>19</sup>S. S. Murzin, Zh. Eksp. Teor. Fiz. **44**, 45 (1986) [Sov. Phys.—JETP **44**, 56 (1986)].
- <sup>20</sup>See M. Shayegan, V. J. Goldman, and H. D. Drew, in *Proceedings of the 18th International Conference on the Physics of Semiconductors, Stockholm, 1986*, edited by O. Engström (World Scientific, Singapore, 1987), p. 1207; G. Nimtz, J. Gebhardt, B. Schlicht, and J. P. Stadler, Phys. Rev. Lett. **55**, 443 (1985); T. F. Rosenbaum, S. B. Field, D. A. Nelson, and P. B. Littlewood, *ibid.* **55**, 444; also see Ref. 12.
- <sup>21</sup>W. N. Shafarman, T. G. Castner, J. S. Brooks, K. P. Martin, and M. J. Naughton, Phys. Rev. Lett. **56**, 980 (1986); D. W. Koon and T. G. Castner, Solid State Commun. **64**, 11 (1987); Phys. Rev. Lett. **60**, 1755 (1988).
- <sup>22</sup>G. A. Thomas, M. J. Burns, P. F. Hopkins, and R. M. Westervelt, Philos. Mag. B **56**, 687 (1987).
- <sup>23</sup>R. M. Westervelt, M. J. Burns, P. F. Hopkins, and A. J. Rimberg, in *Proceedings of the University of Tokyo International Symposium on Anderson Localization* (Springer-Verlag, Berlin, 1988).
- <sup>24</sup>S. M. Sze, *Physics of Semiconductor Devices* (Wiley, New York, 1981), p. 33.
- <sup>25</sup>H. J. Lippmann and U. F. Kuhrt, Z. Naturforsch. **13a**, 462 (1958).
- <sup>26</sup>H. Fritzsche, in *Methods of Experimental Physics*, Vol. 6B of *Solid State Physics*, edited by K. Lark-Horovitz and V. A. Johnson (Academic, New York, 1959), Chap. 8.
- <sup>27</sup>L. J. van der Pauw, Philips Res. Rep. **13**, 1 (1958).
- <sup>28</sup>J. P. Thompson, Philos. Mag. B **38**, 527 (1978).
- <sup>29</sup>G. A. Thomas, Y. Ootuka, S. Katsumoto, S. Kobayashi, and W. Sasaki, Phys. Rev. B **25**, 4288 (1982).
- <sup>30</sup>G. A. Thomas, A. Kawabata, Y. Ootuka, S. Katsumoto, S. Kobayashi, and W. Sasaki, Phys. Rev. B **26**, 2113 (1982).
- <sup>31</sup>S. B. Field and T. F. Rosenbaum, Phys. Rev. Lett. **55**, 522 (1985).
- <sup>32</sup>T. F. Rosenbaum, K. Andres, G. A. Thomas, and P. A. Lee, Phys. Rev. Lett. **46**, 568 (1981).
- <sup>33</sup>T. F. Rosenbaum, R. F. Milligan, G. A. Thomas, P. A. Lee, T. V. Ramakrishnan, and R. N. Bhatt, Phys. Rev. Lett. **47**, 1758 (1981).
- <sup>34</sup>P. F. Hopkins, M. J. Burns, G. A. Thomas, and R. M. Westervelt (unpublished).
- <sup>35</sup>A. Kawabata, Solid State Commun. **34**, 431 (1980).
- <sup>36</sup>B. L. Altshuler, A. G. Aronov, A. I. Larkin, and D. E. Khmel'nitskii, Zh. Eksp. Teor. Fiz. **81**, 768 (1981) [Sov. Phys.—JETP **54**, 411 (1981)].
- <sup>37</sup>M. C. Maliepaard, M. Pepper, R. Newbury, and G. Hill, Phys. Rev. Lett. **61**, 369 (1988).
- <sup>38</sup>M. Rohde and H. Micklitz, Phys. Rev. B **36**, 7572 (1987).
- <sup>39</sup>B. L. Altshuler, D. Khmel'nitskii, A. I. Larkin, and P. A. Lee, Phys. Rev. B **22**, 5142 (1980).
- <sup>40</sup>M. Gruenewald, H. Mueller, P. Thomas, D. Wuertz, Solid State Commun. **38**, 1011 (1981).
- <sup>41</sup>H. Bottger and V. Bryksin, Phys. Status Solidi B **80**, 569 (1977).
- <sup>42</sup>L. Friedman and M. Pollak, Philos. Mag. B **44**, 487 (1981).
- <sup>43</sup>C. J. Adkins, J. Phys. C **11**, 851 (1978).